Journal of Sound and Vibration 329 (2010) 2953–2971

Contents lists available at ScienceDirect

Journal of Sound and Vibration

journal homepage: www.elsevier.com/locate/jsvi

Vibration transmissibility characteristics of the human hand–arm system under different postures, hand forces and excitation levels

S.A. Adewusi [a], S. Rakheja [a], P. Marcotte [b,*], J. Boutin [b]

[a] CONCAVE Research Center, Concordia University, 1455 de Maisonneuve West, Montréal, Québec, Canada H3G 1M8
[b] Institut de recherche Robert-Sauvé en santé et en sécurité du travail, 505 de Maisonneuve West, Montréal, Québec, Canada H3A 3C2

ARTICLE INFO

Article history:
Received 22 July 2009
Received in revised form
2 February 2010
Accepted 3 February 2010
Handling Editor: H. Ouyang
Available online 26 February 2010

ABSTRACT

Biodynamic responses of the hand–arm system have been mostly characterized in terms of driving-point force-motion relationships, which have also served as the primary basis for developing the mechanical-equivalent models. The knowledge of localized vibration responses of the hand–arm segments could help derive more effective biodynamic models. In this study, the transmission of z_h-axis handle vibration to the wrist, elbow and the shoulder of the human hand and arm are characterized in the laboratory for the bent-arm and extended arm postures. The experiments involved six subjects grasping a handle subject to two different magnitudes of broad-band random vibration, and nine different combinations of hand grip and push forces. The vibration transmissibility data were acquired in the z_h- and y_h-axis at the wrist and shoulder, and along all the three axes around the elbow joint. The results show that the human hand–arm system in an extended arm posture amplifies the vibration transmitted to the upper-arm and the whole-body at frequencies below 25 Hz, but attenuates the vibration above 25 Hz more effectively than the bent-arm posture, except at the shoulder. The magnitudes of transmitted vibration under an extended arm posture along the y_h-axis were observed to be nearly twice those for the bent-arm posture in the low frequency region. The results further showed that variations in the grip force mostly affect vibration transmissibility and characteristic frequencies of the forearm, while changes in the push force influenced the dynamic characteristics of the entire hand–arm system. The magnitudes of transmitted vibration in the vicinity of the characteristic frequencies were influenced by the handle vibration magnitude.

1. Introduction

Clinical and epidemiological studies have shown that operators of hand-held power tools are prone to develop various vibration-induced disorders of the hand and arm, which are collectively referred as hand–arm vibration syndrome (HAVS) [1–3]. Considerable efforts have been made to enhance understanding of the human hand–arm responses to vibration and the phenomenon of HAVS, which include the epidemiological studies [1–6], dose-response relation [7], measurement and assessment of vibration dosage [8,9], hand–tool interactions [10,11], control of hand-transmitted vibration (HTV) [12–15], and the human hand–arm responses to HTV [16–18]. The hand–arm responses to vibration have been mostly investigated in terms of biodynamic responses, which are believed to serve as the essential foundation for understanding

* Corresponding author. Tel.: +1 514 288 1551x251; fax: +1 514 288 9399.
E-mail address: marcotte.pierre@irsst.qc.ca (P. Marcotte).

0022-460X/$ - see front matter © 2010 Elsevier Ltd. All rights reserved.
doi:10.1016/j.jsv.2010.02.001

the mechanisms associated with vibration-induced disorders and for developing better risk assessment methods [19,20]. Moreover, thorough characterizations of the biodynamic responses are considered vital for design and assessment of vibration attenuation devices, and for developing hand–arm vibration simulators for assessment of power tools [21,22].

The biodynamic responses of the human hand–arm system to vibration have been mostly characterized using three methods based on: (i) force-motion relationship at the hand–tool interface, expressed in terms of driving-point apparent mass (AM) or driving-point mechanical impedance (MI) or vibration power absorption (VPA) [16,17,23]; (ii) vibration transmitted to different segments of the hand–arm system, such as the nail, finger, wrist, elbow and shoulder [24–31]; and (iii) mechanical-equivalent models that are mostly derived from the driving-point measures [21,32]. The vast majority of studies have reported the force-motion relation in terms of MI, due to relative ease of its measurement. These studies have provided considerable knowledge related to various influencing factors, such as handle size, grip and push forces, hand–arm posture, and direction and magnitude of vibration. The ranges of impedance responses to x_h-, y_h- and z_h-axis vibration have also been defined in the International Standard, ISO 10068 [33] on the basis of a synthesis of the reported driving-point mechanical impedance data [34].

The responses measured at the hand–handle driving-point have been applied to derive total vibration energy absorbed into the hand–arm system, important resonant frequencies and mechanical-equivalent models. The driving-point measures, however, cannot fully describe the distributed vibration responses of the hand–arm system, particularly the vibration modes associated with the forearm and the upper-arm, and their contribution to the driving-point responses. It has been suggested that the vibration responses of individual segments or distribution of vibration energy within the hand–arm structure could provide better assessment of vibration-induced injury risks [35,36].

Characterization of distributed responses necessitates development of reliable mechanical-equivalent models based on representative anatomical structure of the hand–arm system. The vast majority of the models, however, have been developed using the mechanical impedance measure and do not represent anatomical structure of the hand–arm system to predict biodynamic responses. A recent study proposed a biodynamic model for simulating biodynamic responses distributed at the fingers and the palm of the hand under z_h-axis vibration by introducing two driving-points formed by the fingers–handle and palm–handle interfaces [36,37]. The model parameters were identified solely from the driving-point impedance measured on the palm- and fingers- sides of the hand, while the vibration power absorption within different segments was estimated from the model. The quality of such a model could be considerably enhanced with knowledge of vibration responses of different substructures of the hand and arm, particularly with consideration of the anatomical structure. The vibration transmitted along the hand–arm structure could also yield insight into additional vibration modes and their contributions to the overall driving-point measures. The mechanical-equivalent model, realized on the basis of the distributed vibration responses, apart from the localized impedance, could then yield more reliable prediction of the distributed VPA for exposure risk assessments.

Only a few studies have reported vibration transmissibility responses of the human hand–arm system [24–31], which is perhaps partly attributed to complexities associated with measurement of vibration on the human skin, and small magnitudes of transmitted vibration above 200 Hz. There are considerable discrepancies among the reported transmissibility responses and the effect of excitation level on transmissibility. These may be attributed to different measurement methods and experimental conditions such as location of accelerometer, excitation magnitude and direction, frequency range, grip force, posture, subjects' anthropometry and handle diameters, as shown in Table 1. The studies also differ on the resonant frequencies of the human hand–arm system and the method of their identification, although the majority did not attempt to identify the resonance frequencies due to lack of conspicuous magnitude peaks. The frequencies corresponding to the valleys in the magnitude response were reported as the resonant frequencies [27], while those corresponding to peaks in the imaginary component of the transmissibility function were reported as resonant frequency in [29]. The first three natural frequencies were expressed in terms of the grip force in [29]. Furthermore, somewhat contradictory findings have been reported in the reported transmissibility studies on the effects of the excitation magnitudes. Two studies have reported that a 10 dB increase in the excitation magnitude increases the transmissibility by 8–10 dB at all frequencies [27,30], while negligible influence of excitation magnitude on the wrist transmissibility was reported in [29].

Despite the observed differences, all of the reported data consistently show rapid decrease in the vibration transmissibility of the hand–arm segments with increasing frequency and distance from the source of vibration and useful conclusions have been reported. For examples, it was reported that vibration attenuation occurs in the tissue adjacent to the bone and only little vibration attenuation occurs across the joints even though large relative motion across joints could be observed [26]. The vibration at frequencies below 100 Hz could be transmitted to the forearm, and that below 40 Hz was transmitted to the upper arm [27]. Similar to observation from impedance responses, vibration above 200 Hz is confined to the hand [26,27,29]. An increase in the grip force increased the resonance frequency [29]. The reported data suggest the presence of characteristic frequencies, corresponding to peaks in the transmissibility responses, within the 7–16, 30–50, 65–80, 90–140, and 150–200 Hz bands; some of these compare reasonably well with the resonant frequencies observed from the mechanical impedance responses [23,41]. The measurement of the head vibration using a bite-bar revealed considerable head vibration in the 12.5–16 Hz bands under an extended arm posture [30]. The observed high vibration of the head in [30] raises concern on the validity of the majority of the mechanical-equivalent models of the hand–arm system that include a fixed support at the shoulder.

Table 1
Summary of experimental conditions employed in studies reporting hand–arm vibration transmissibility.

Investigator	Acceleration Measurement		Excitation		Frequency range (Hz)	Grip force	Elbow angle	Handle diameter
	Locations	Method	Type and direction	Magnitude				
Kihlberg [24]	Finger, wrist and elbow	Accelerometers mounted on plastic sheet and taped to locations	Grinder vibration z_h					
	Reference	Handle		NR[a]	20–1000	50 N	110°	NR[a]
Kattel and Fernandez [25]	Wrist, elbow and shoulder	Accelerometers on hand adapter and bracelets	Rivet gun z_h			18 N		
	Reference	Handle		NR[a]	NR[a]	26 N	90°	NR[a]
Reynolds and Angevine [26]	Finger, wrist, elbow and shoulder	Accelerometer attached to skin using adhesive tape	Sinusoidal x_h, y_h, z_h			9 N		
	Reference	Handle base		NR[a]	5–1000	18 N	NR[a]	19 mm
Pyykko et al. [27]	Wrist, elbow and upper arm[b]	Accelerometer mounted on plexiglass attached to location by a metal clamp with screws	Sinusoidal z_h	1, 3 and 10 g rms		10 N		
	Reference	Handle			20–630	20 N 40 N	120°	25 mm
Cherian et al. [28]	Finger and elbow	Accelerometer attached on a ring for the middle finger; and on an aluminum strip held by an elbow pad	Sinusoidal z_h					
	Reference	Handle base		0.5 g peak	10–200	25 N	90°	38 mm
Aatola [29]	Wrist	Accelerometer attached on acrylic plate held tight by hose clamp	Sinusoidal z_h	2.5, 7.9 and 25 ms^{-2}		10 to 40 N		
	Reference	Handle			10–300		150°	26 mm
Sakakibara et al. [30]	Head	Accelerometer attached on a bite-bar	Sinusoidal x_h	3.15, 10.1, 31.5 ms^{-2}		5 kg		
	Reference	Handle			8–200		180°	NR[a]
Xu et al. [31]	Wrist and Elbow	Tri-axial accelerometers attached to the skin with medical tape	Broadband random	3.0 $(ms^{-2})^2$/Hz	6.3–400	NR[a]	About 90°	NR[a]
	Reference	Handle			1/3 octave			

[a] Not reported.
[b] In the vicinity of the elbow, medial epicondylus.

However, the effect of push force on the transmitted vibration has not been investigated, which is known to have notable effect on the low frequency impedance responses [23]. Therefore, there is need for further systematic measurements of the vibration transmissibility responses of the hand–arm system under a range of important influencing factors, namely the grip force, push force, posture and the vibration level. The resulting data of the distributed vibration properties could help derive more reliable models capable of predicting distributed vibration power absorption and localized deformations for assessment of potential exposure risks.

In this study, laboratory experiments were performed to obtain estimates of transmission of z_h-axis handle vibration to the underlying bone/joint structures of the wrist, elbow and the shoulder of the human hand–arm system under different combinations of grip and push forces, excitation magnitudes and two different postures. The measured data are analyzed to study the contributions of primary influencing factors to the magnitudes of transmitted vibration and the resonant frequencies using the statistical analysis of variance (ANOVA). The primary hypothesis of this study is that characterization of vibration transmitted along the hand–arm structure could yield considerable insight into the hand–arm vibration modes, and the influences of important operating factors such as posture, hand forces and vibration level. The vibration responses could provide essential target functions for development of mechanical-equivalent models on the basis of the distributed vibration responses, apart from the localized driving-point impedance, which would yield more reliable predictions of distributed vibration power absorption for exposure risk assessments.

2. Methods

2.1. Experimental set-up

Laboratory experiments were performed to measure vibration transmitted to the wrist, elbow and shoulder of the dominant right hand and arm of six adult male subjects in the standing position, while grasping a 40 mm diameter handle subject to z_h-axis vibration. The experiments were conducted with two different hand–arm postures (P1—bent-arm with 90° elbow angle; P2—extended arm with 180° elbow angle), three different grip forces (F_g=10, 30 and 50 N) and push forces (F_p=25, 50, 75 N), and two different magnitudes of broad-band random vibration in the 2.5–2500 Hz frequency range with constant power spectral density (a_{hw}=2.65 and 5.25 ms^{-2}). Various physical dimensions of the hand–arm of the subjects were measured. The mean and ranges of these dimensions together with the subject weight, height, age and body mass index (BMI) are summarized in Table 2.

An instrumented 40 mm diameter cylindrical handle, described in [23], was used in this study. The handle comprised two Kistler force sensors to measure the grip force, while two additional force sensors were installed between the handle support brackets and the base fixture for measurement of the push and total dynamic force. The handle with base fixture was installed on an electrodynamic shaker. The measured grip and push forces were low-pass filtered and displayed to the subjects at a rate of 4 samples per second so as to allow the subjects to maintain the hand forces in the desired ranges. A PCB SEN026 tri-axial accelerometer was installed inside the handle, while the signal along the z_h-axis alone was acquired. The vibration transmitted to four different locations on the hand–arm were measured using tri-axial PCB accelerometers attached to Velcro strips (Fig. 1), which were tightly fastened near the joints so as to minimize the contributions due to skin artifacts, while corrections for the skin deformation were not attempted. The locations included the wrist, shoulder and near the elbow joints on the forearm and upper-arm sides, referred to as 'elbow 1' and 'elbow 2', respectively, as shown in Figs. 1(a) and (b). Care was taken to ensure that Velcro strips were neither loose nor too tight to allow free flow of blood and subjects' comfort. Accelerations along the y_h- and z_h-axes were measured at the wrist and shoulder, while accelerations near the elbow joint were measured along all the three directions, following the basicentric coordinate system recommended in [19]. Orientation of the accelerometers mounted on the upper-arm, however, change with

Table 2
Ranges of hand–arm dimensions and physical properties of six subjects.

Parameter	Range	Mean	Standard deviation
Age (years)	26–53	36.5	11.3
Height (m)	1.71–1.80	1.74	0.02
Weight (kg)	61–86	72.2	9.9
BMI	20.4–28.7	23.8	3.1
Hand length (cm)	17.0–20.5	18.4	1.2
Hand breath at thumb (cm)	9.5–12.0	10.9	0.9
Hand breath at metacarpal (cm)	7.0–8.5	7.5	0.6
Hand thickness (cm)	2.0–3.7	2.9	0.6
Wrist diameter (cm)	16.0–18.5	17.3	1.0
Forearm diameter (cm)	25–32	28.0	2.5
Elbow diameter (cm)	24.4–30.5	26.4	2.2
Forearm length (cm)	24.0–28.5	26.0	1.6
Upper arm diameter (cm)	28–33	29.3	3.1
Upper arm length (cm)	18–24	20.5	2.4

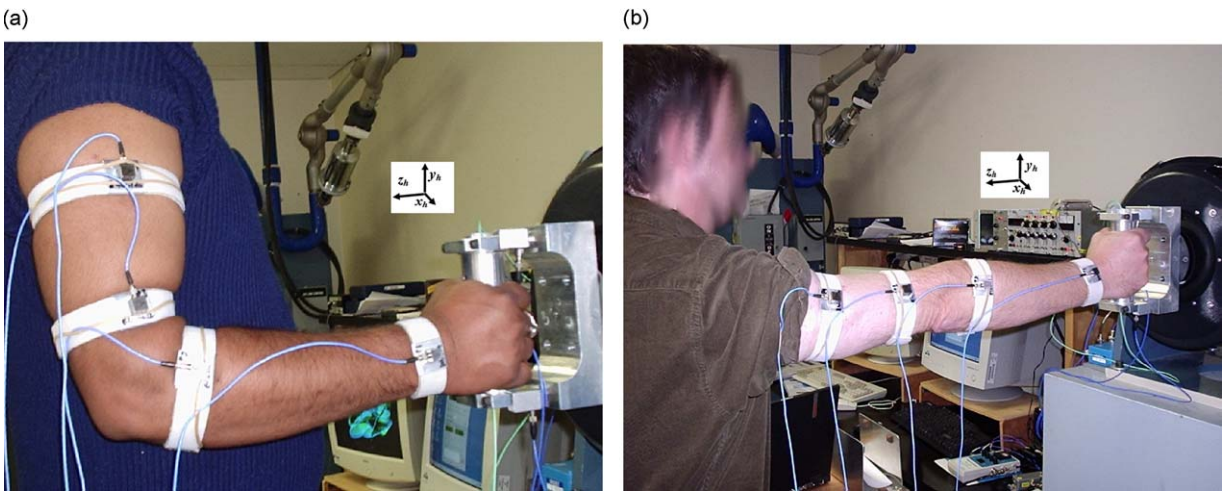

Fig. 1. Experimental set-up: (a) bent-arm posture (P1); (b) extended arm posture (P2).

posture. The z_h- and y_h-axis of the accelerometers in the bent-arm posture become oriented along the y_h- and z_h-axis, respectively, for the extended arm posture. Considering the small mass of tissues/muscles at the wrist and that the Velcro strips were tightly fastened around the hand–arm at the measurement locations, the transmissibility at the wrist is considered a good estimate of the underlying bone/joint structure. The larger mass of muscles/tissues on the upper-arm, which are stiffened under grip and push forces, may affect transmissibility estimates obtained on the upper-arm.

Each subject was advised to grip and push the handle assuming selected posture, while maintaining the desired hand forces within ± 2 N by monitoring the displayed forces on a monitor. The handle was subsequently vibrated and the measured signals from the handle as well as response accelerometers were acquired in a 01 dB multi-channel data acquisition system. During the experiments, the hand–arm posture was visually monitored by the experimenter to ensure the desired posture and orientations of the accelerometers. The coherence of the measurements was also monitored during the experiments to ensure reliability of the measured data. Each measurement lasted for 8 s and was repeated three times, while the order of the hand forces combinations was randomized for each posture. These were later examined to study the repeatability and inter-subject variability. The reproducibility of the measurements was also evaluated with two subjects by removing and re-fastening the Velcro strips containing the response accelerometers after each run under bent-arm posture, 30 N grip force and 50 N push force.

2.2. Data analysis

The measured data were analyzed to derive characteristics of vibration transmitted to the measurement locations in terms of vibration transmissibility, using the H_1 frequency response estimator. The analysis was performed using a bandwidth of 2500 Hz with frequency resolution of 0.78 Hz, and an overlap of 75%. The reproducibility of the measurements attained with two subjects was evaluated in terms of mean data of the trials for two runs, and the deviation of the means was used to evaluate the effect of variability in the tightness of the strap. The intra-subject variability of the measurements was also evaluated in terms of peak standard deviation of the mean data of the trials. The mean transmissibility values of the three trials for the subjects were used to determine the inter-subject variability in a similar manner. The characteristic frequencies were identified as those corresponding to the peaks in the mean measured transmissibility. A number of studies on modal analyses of simples systems have shown that peaks in transmissibility correspond to the system resonant frequencies for output–input frequency response function [39,40]. The effects of different experimental conditions on the transmitted vibration at each location were evaluated from the mean transmissibility responses, and through Analysis of Variance (ANOVA) using the Statistical Product and Service Solutions (SPSS) software. The main factors included the grip force, push force and vibration magnitude for each hand–arm posture. The analyses were performed with the data at eight discrete frequencies close to some of the characteristic frequencies identified from the mean measured transmissibility magnitudes. Multivariate ANOVA using the general linear model (GLM) technique was used to study the influence of the main factors for each posture on both z_h- and y_h-axis vibration transmissibility. The transmissibility measured at the wrist (W), elbow 1 (E1), elbow 2 (E2) and shoulder (S) were considered as the dependent variables. The significant values of the analysis correspond to 95% confidence intervals (α=0.05). The reliability of statistical analysis is dependent upon the total sample size involving the number of subjects, the number and levels of the factors (independent variables) considered, the variability of experimental data, the required confidence level, and the magnitude of the effect to be detected [47,48]. In this study, the ANOVA design for each posture and direction involved three factors (independent variables) namely: two levels of excitation magnitude, three levels of

grip force and three levels of push force, resulting into a total sample size of 108. The "power of the *F*-test", which measures the acceptability of the ANOVA results [48], was also computed for each analysis at each discrete excitation frequency considered. The results attained consistently revealed the power value in the excess of 0.9, well above the acceptable value of 0.8 for analysis to be considered valid [48].

3. Results and discussions

3.1. Repeatability and reproducibility of measurements

The repeatability of the data acquired with each subject was investigated for the bent-arm (P1) posture with 30 N grip and 50 N push hand forces. The selected hand forces are identical to those recommended in ISO 10819 [42] for the assessment of anti-vibration gloves. Moreover, this hand forces combination was judged as the most comfortable and easily controllable by all the subjects. Comparisons of repeated measurements, for all locations, revealed reasonably good agreements for all subjects. As an example, Figs. 2(a) and (b) show the comparison of the three measurement trials obtained with one of the subjects at the elbow (E2) location along the z_h- and y_h-axis, respectively. The measurements revealed peak standard deviation (SD) in the z_h-axis transmissibility magnitude at the wrist of 0.37 near 39 Hz, where the mean value was in the order of 1.41. The coherence in the z_h-axis measurement was nearly unity up to 200 Hz, but considerably lower near 300 and 600 Hz, which may be attributed to lower magnitudes of transmitted vibration at higher frequencies, since high frequency vibration is confined to the hand. The y_h-axis transmissibility data also revealed lower coherence at frequencies above 500 Hz.

The reproducibility of the measurements was evaluated through analysis of data acquired with two subjects. The comparisons of means and peak standard deviations of two runs involving removal and re-installation of Velcro strips at different locations revealed reasonably good agreements, irrespective of the measurement location. For instance, the peak SD of the mean z_h-axis wrist transmissibility attained during two runs ranged from 0.26 to 0.37 and 0.24 to 0.26 in the 35–39 Hz band for the two subjects. The corresponding mean values of the two runs were in the order of 1.99–1.42 and 1.53–1.88 for the two subjects. The observed values of standard deviations were considered to be comparable, which suggest that the Velcro strap-mounted accelerometer could yield reproducible measurements despite possible variations in the tightness and slight deviation of the accelerometers from the intended orientation. Considering the extremely low transmissibility magnitudes above 500 Hz, the subsequent analysis of the data were limited to 2.5–500 Hz frequency range, although a number of studies have reported transmitted vibration up to frequencies as high as 1000 Hz [24,26].

3.2. Inter-subject variability

The mean responses attained for the six subjects revealed considerable inter-subject variations. As examples, Figs. 3 and 4 illustrate the mean wrist and shoulder vibration transmissibility responses acquired with the bent-arm posture together

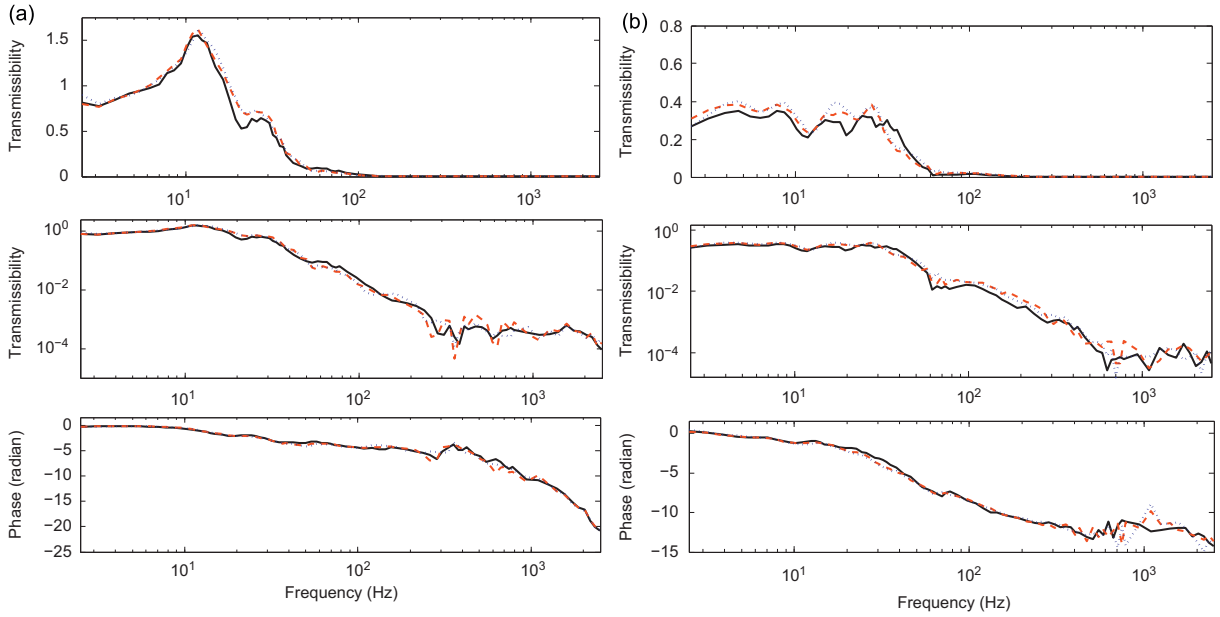

Fig. 2. Comparisons of acceleration transmissibility measured at elbow 2 of one subject during the three trials (bent-arm posture (P1), F_g=30 N, F_p=50 N and a_{hw}=5.25 ms^{-2}): (a) z_h-axis; (b) y_h-axis.

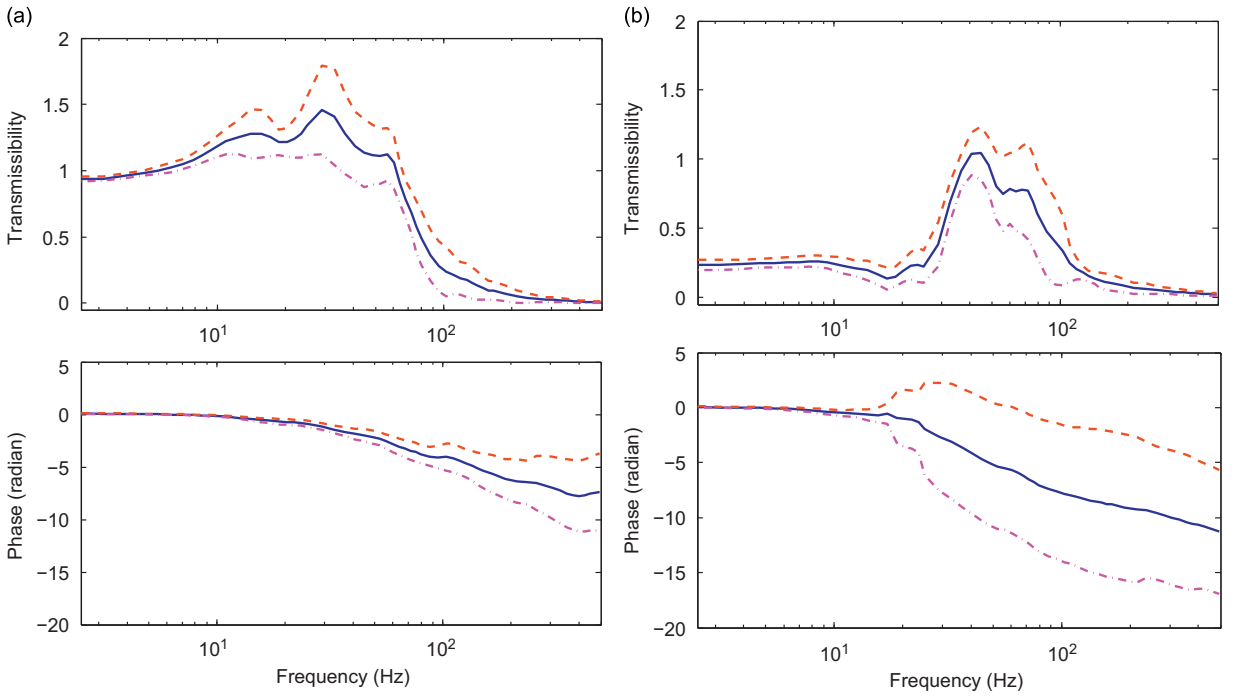

Fig. 3. Mean and standard deviation (SD) of mean vibration transmissibility measured at the wrist (bent-arm posture, F_g=30 N, F_p=50 N and a_{hw}=5.25 m/s^2): (a) z_h-axis; (b) y_h-axis; mean; mean+SD; mean−SD.

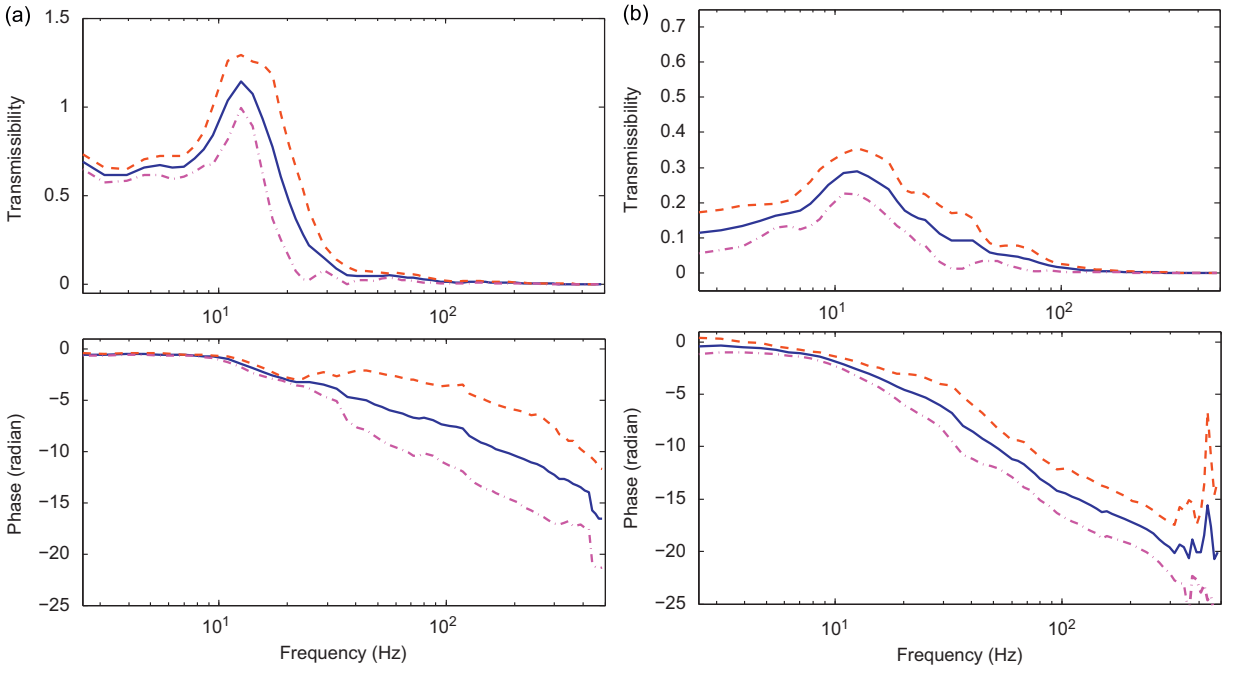

Fig. 4. Mean and standard deviation (SD) of mean vibration transmissibility measured at the shoulder (bent-arm posture, F_g=30 N, F_p=50 N and a_{hw}=5.25 ms^{-2}): (a) z_h-axis; (b) y_h-axis; mean; mean+SD; mean−SD.

with the standard deviation (SD). These results were obtained under F_g=30 N, F_p=50 N and a_{hw}=5.25 m/s^2. The transmissibility responses of the six subjects in the direction of excitation, z_h-axis, generally revealed comparable trends but higher deviations could be observed around the transmissibility peaks. This may be associated with differences in biodynamic and anthropometric properties of the subjects. The responses in the y_h-axis revealed relatively larger variations and lower magnitudes. The dispersions in the x_h-axis responses around the elbow were observed to be large,

while the magnitudes were comparable with those of y_h-axis transmissibility (the results not shown). The peak deviations of the mean z_h-axis measurements were obtained as 0.37 at 32.8 Hz for the wrist, 0.26 at 28.9 Hz for elbow E1, and 0.41 at 17.2 Hz for both the elbow E2 and the shoulder locations. The mean values at these frequencies were in the order of 1.41, 1.40, 1.20 and 0.77, respectively. The phase responses reveal relatively larger deviations at frequencies above 200 Hz, as shown in Figs. 3 and 4.

The observed variabilities in the magnitude and phase data acquired with six subjects appear to be considerably lower than those reported in [26,29]. These studies, however, did not report the inter-subject variabilities of the measured data, while the observed substantial scatter in the data was attributed to variations in the hand-grip force during the test. Apart from the hand force variations, the differences in biodynamic and anthropometric parameters of individuals, and possible variations in the posture and orientation of accelerometers could contribute to greater inter-subject variability. The vibration transmissibility responses attained with the extended arm posture also revealed comparable values of inter-subject variability, while greater deviations occurred below 25 Hz.

3.3. Mean vibration transmissibility responses

Figs. 5 and 6 illustrate the mean transmitted vibration magnitude and phase responses for both postures measured at the wrist, elbow (E1 and E2) and shoulder along the z_h- and y_h-axis, respectively, for both postures (F_g=30 N, F_p=50 N and a_{hw}=5.25 m/s^2). The mean vibration transmissibility measured along the x_h-axis at E1 and E2 were observed to be comparable with those along the y_h-axis for both the postures, and are not presented. The mean transmissibility is presented in both the linear and logarithmic scales in order to illustrate the response variations in low and high frequency ranges, respectively. The results further show the widely different low frequency transmissibility responses at different locations, when the mean data are observed in the linear scale. These differences are not evident in the logarithmic scale presentation, while the differences in transmissibility at frequencies above 100 Hz are evident only in the logarithmic scale. The z_h-axis transmissibility for the bent-arm posture generally decreases with increasing distance from the driving-point, although the transmissibility at the elbow (E1 and E2) is higher than that of the wrist around 12.5 Hz. This is evident only in the linear scale representation of the data and may be attributed to the resonance of the upper arm near 12.5 Hz. The y_h-axis transmissibility under the bent-arm posture is considerably lower than that in the z_h-axis, as seen in Fig. 6(a). The y_h-axis transmissibility above 30 Hz also tends to decrease with increasing distance from the driving-point, as observed from the z_h-axis responses. The z_h- and y_h-axis transmissibility phase decreases with increasing frequency. The wrist and elbow transmissibility phase responses are generally comparable, while that of the shoulder tends to be considerably lower.

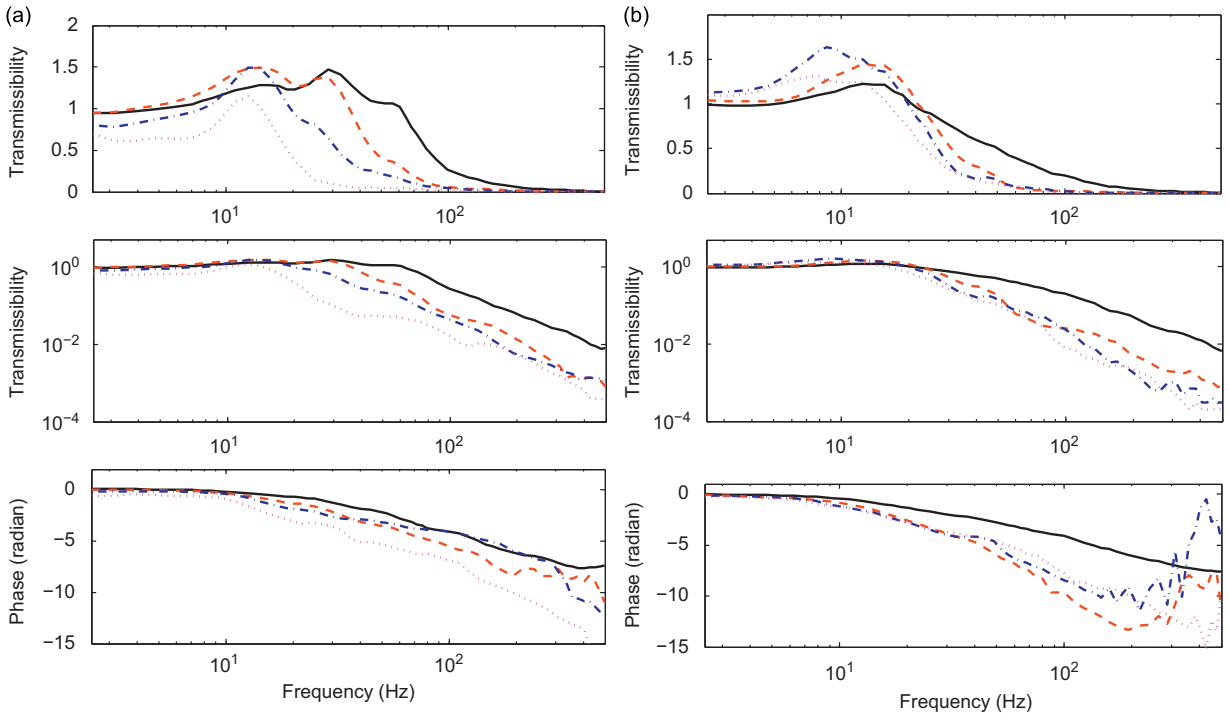

Fig. 5. Comparisons of z_h-axis mean transmissibility responses measured at different locations (F_g=30 N, F_p=50 N and a_{hw}=5.25 ms^{-2}): (a) bent-arm posture (P1); (b) extended arm posture (P2); ——— wrist; — — elbow 1; - - - - elbow 2; ·····shoulder.

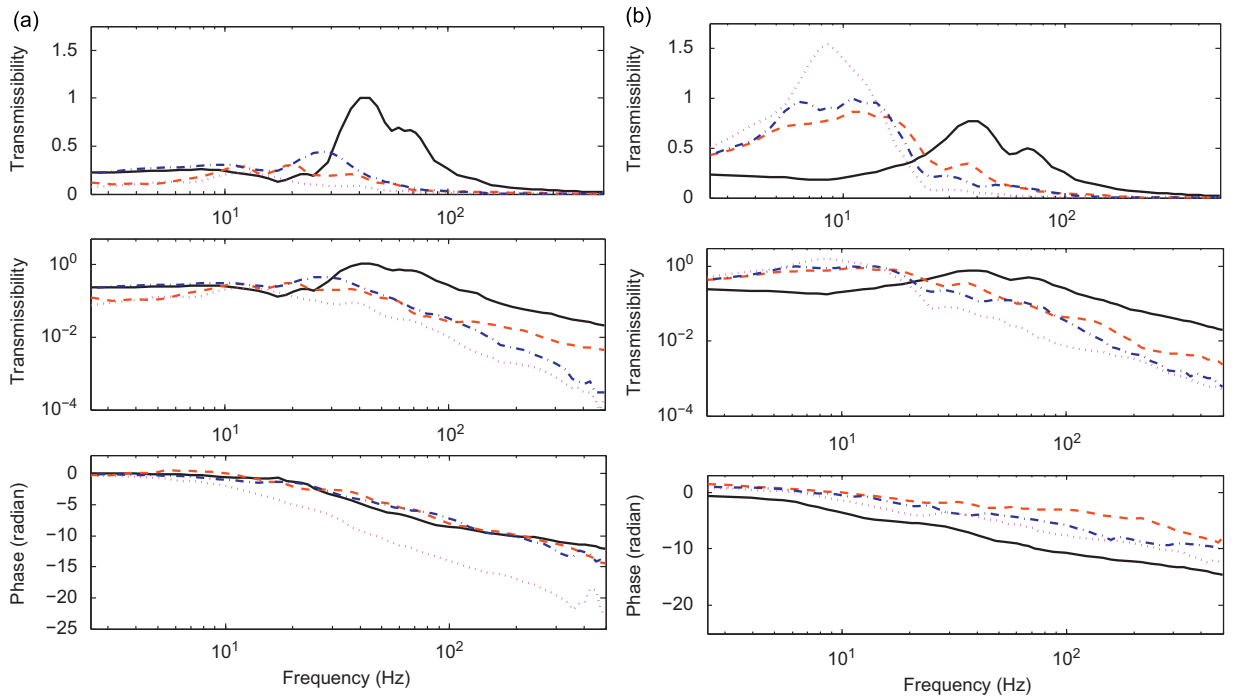

Fig. 6. Comparisons of y_h-axis mean transmissibility responses measured at different locations (F_g=30 N; F_p=50 N and a_{hw}=5.25 ms^{-2}); (a) bent-arm posture (P1); (b) extended arm posture (P2); wrist; elbow 1; elbow 2; shoulder.

Unlike the bent-arm (P1) posture, the z_h-axis transmissibility at the elbow and shoulder is considerably larger than that at the wrist for the extended arm (P2) posture in the 2.5–25 Hz frequency range, as seen in Fig. 5(b). The transmissibility at frequencies above 25 Hz, however, is lower with increasing distance from the driving-point, as observed for the bent-arm posture. Furthermore, the low frequency transmissibility (below 15 Hz) is either greater than or equal to 1.0, irrespective of the measurement location, suggesting greater transmission of the low frequency vibration under the extended arm posture. Such differences, however, are not evident from the logarithmic scale presentation of the responses, as evident in Fig. 5. The mean y_h-axis responses under the P2 posture (extended arm) are also considerably different from those acquired under the P1 posture (bent arm), as seen in Fig. 6, and they are considerably lower than those in the z_h-axis. Unlike the P1 posture, the y_h-axis transmissibility at the shoulder and elbow for the P2 posture are considerably larger than that at the wrist. This suggests greater low frequency y_h-axis vibration of the upper arm structure under the extended arm posture.

The difference in the wrist transmissibility for the two postures is very small below 20 Hz compared to the other measurement locations, which suggests that the low frequency vibration transmitted to the wrist is less sensitive to postural variations. The extended arm posture, however, yields lower z_h- and y_h-axis wrist vibration than the bent-arm posture at frequencies above 25 Hz. The y_h-axis vibration transmitted to the elbow (E1 and E2) and the shoulder under the extended arm posture are larger than those for the bent-arm posture below 25 Hz. The results generally show considerably lower y_h- and z_h-axis vibration of the upper arm for the bent-arm posture than the extended arm posture. The extended arm posture also causes considerable low frequency vibration of the head in the 12.5–16 Hz frequency range [30]. Similar to the observed effect of posture on low frequency transmissibility, the apparent mass and impedance responses of the hand–arm system also revealed greater sensitivity to the posture in the low frequency range. It has been shown that the extended arm posture yields considerably larger low frequency apparent mass and impedance due to stronger coupling between the hand and the handle [16]. The mean vibration transmissibility (Figs. 5 and 6) show that the extended arm posture causes greater transmission of the z_h-axis source vibration to the upper-arm and thus the trunk below 25 Hz, while it attenuates vibration above 25 Hz more effectively than the bent-arm posture. This suggests that a greater proportion of the medium to high frequency vibration under the extended arm posture may be limited to the hand. A number of studies have shown that the vibration above 150 Hz is limited to the hand under the bent-elbow posture [28,31]. The extended arm posture may thus impose greater risk of musculoskeletal disorders than the bent-arm posture under exposure to low frequency power tools and greater risk of vibration-induced white finger under exposure to high frequency power tools.

The mean vibration response magnitudes measured along the x_h-, y_h- and z_h-axis were examined to identify the characteristic frequencies corresponding to peaks in transmissibility. The measured data revealed that most prominent transmissibility peaks occur consistently in the 5.5–7.0, 10.9–12.5, 20.3–28.9, 40.6–44.5, $\approx$56.3, 68.0–71.6, 134.4–157.8 and 216.4–239.8 Hz ranges for the bent-arm posture and in the 6.3–8.9, 10.9–15.6, 25.0–28.9, 36.7–48.4, 64.1–68.0, 110.9–134.4 and 200.0–216.0 Hz for the extended arm posture. Some of the ranges of resonant frequencies derived

from the measured transmissibility are comparable with those observed from the reported studies summarized in Table 1. The first three resonant frequencies of the human hand–arm system, corresponding to 30 N grip force, are 31, 138 and 201 Hz using the expression defined in [29].

The mean transmissibility for the six subjects are subsequently analyzed to study the effects of grip and push forces, and the excitation magnitudes for both postures. Statistical analyses (ANOVA) are also performed on the data in the vicinity of the identified characteristics frequencies and a slightly higher frequency of 300 Hz. Tables 3 and 4 summarize the statistical significance (p-values) of the main effects (F_g, F_p and a_{wh}) on the z_h- and y_h-axis transmitted vibration, respectively, for both postures.

3.4. Comparisons of the measured transmissibility with the reported studies

Fig. 7 illustrates comparisons of the mean measured transmissibility, for both the bent-arm and extended arm postures, and a few selected transmissibility data sets from reported studies at the wrist and elbow. The data reported in [25] are excluded since these were limited to overall rms values of acceleration measured at different locations. Furthermore, the transmissibility of the head and the shoulder are not compared since these were reported in a single study [30,26]. Owing to very small magnitudes of the transmissibility at frequencies above 100 Hz, the responses are also illustrated in the logarithmic scale, while the results in the linear scale are shown to emphasize the variations at lower frequencies.

The figure shows that the mean measured wrist and elbow transmissibility responses for the bent-arm posture are quite comparable with those reported in a recent study [31]. This suggests that the results of the present study are reliable.

Table 3
Statistical significance of the main factors on transmissibility in the z_h-axis for each posture.

Factors	Location	4.7 Hz		7.8 Hz		14.8 Hz		28.9 Hz		64 Hz		134.4 Hz		200 Hz		300 Hz	
		P1[a]	P2[b]	P1	P2	P1	P2	P1	P2	P1	P2	P1	P2	P1	P2	P1	P2
Grip force	Wrist	0.27	0.83	*0.07*	0.58	0.75	*0.00*	*0.00*	*0.00*	*0.00*	*0.00*	*0.05*	0.47	0.45	0.80	*0.01*	0.95
	Elbow1	0.30	0.35	*0.03*	0.33	*0.05*	*0.00*	*0.00*	*0.00*	*0.01*	0.40	0.11	*0.01*	0.17	*0.00*	*0.00*	0.13
	Elbow2	0.76	0.75	0.34	0.75	*0.00*	*0.00*	*0.00*	*0.00*	0.14	0.07	*0.04*	0.68	*0.00*	0.54	0.80	0.11
	Shoulder	0.99	0.58	0.94	0.56	0.82	*0.00*	0.75	0.17	0.38	*0.02*	*0.00*	0.07	*0.00*	*0.00*	0.45	0.24
Push force	Wrist	*0.00*	0.93	*0.00*	0.47	0.08	*0.00*	0.40	*0.00*	*0.00*	*0.00*	*0.00*	*0.03*	0.13	0.24	0.07	*0.04*
	Elbow1	0.35	0.10	*0.01*	0.25	0.10	*0.00*	*0.00*	*0.00*	*0.00*	*0.05*	0.08	0.24	0.07	0.81	*0.00*	0.74
	Elbow2	*0.03*	0.18	*0.01*	0.73	*0.00*	*0.00*	*0.00*	*0.00*	*0.00*	*0.00*	*0.00*	*0.00*	*0.00*	0.06	*0.01*	0.32
	Shoulder	0.22	0.19	0.10	0.74	0.26	*0.00*	*0.00*	*0.03*	*0.01*	*0.00*	0.14	*0.00*	0.13	*0.00*	*0.02*	0.16
Excitation level	Wrist	0.13	0.41	0.32	0.32	*0.03*	0.60	0.60	0.19	*0.00*	*0.00*	*0.00*	0.23	0.83	0.68	*0.02*	0.19
	Elbow1	*0.00*	*0.05*	*0.02*	0.95	0.14	0.66	0.94	0.95	0.20	*0.01*	0.10	0.26	*0.02*	*0.04*	*0.00*	0.81
	Elbow2	0.95	0.91	0.85	0.49	0.64	0.21	*0.02*	*0.01*	0.52	0.24	0.87	*0.03*	0.95	0.36	*0.00*	0.18
	Shoulder	*0.01*	0.38	0.19	0.26	0.08	0.09	0.07	0.17	0.09	0.10	*0.00*	*0.02*	0.26	0.28	0.63	0.68

[a] Bent-arm (P1) posture.
[b] Extended arm (P2) posture.

Table 4
Statistical significance of the main factors on transmissibility in the y_h-axis for each posture.

Factors	Location	4.7 Hz		7.8 Hz		14.8 Hz		28.9 Hz		64 Hz		134.4 Hz		200 Hz		300 Hz	
		P1[a]	P2[b]	P1	P2	P1	P2	P1	P2	P1	P2	P1	P2	P1	P2	P1	P2
Grip force	Wrist	0.14	0.62	0.22	*0.00*	0.59	*0.00*	*0.05*	0.67	0.30	0.77	*0.03*	*0.00*	0.18	*0.00*	0.14	*0.02*
	Elbow1	0.45	0.56	0.32	0.76	0.31	*0.00*	0.23	*0.02*	*0.01*	*0.00*	*0.01*	*0.00*	0.12	*0.00*	0.07	0.12
	Elbow2	0.82	0.46	0.76	0.13	0.15	*0.00*	0.18	*0.00*	0.19	0.66	0.11	0.68	*0.01*	0.91	0.23	0.54
	Shoulder	0.90	0.24	0.89	0.08	*0.04*	*0.01*	0.41	*0.00*	0.40	0.37	0.80	0.12	0.42	*0.02*	0.17	0.59
Push force	Wrist	*0.00*	0.72	*0.01*	0.18	0.35	0.74	0.42	0.19	*0.00*	0.08	0.97	0.41	0.79	0.61	0.61	0.27
	Elbow1	*0.00*	0.29	*0.00*	0.29	0.82	*0.00*	0.37	*0.03*	*0.00*	*0.00*	*0.04*	*0.00*	0.69	*0.03*	0.40	0.57
	Elbow2	0.82	*0.05*	0.72	0.15	0.25	*0.00*	0.42	*0.00*	*0.01*	*0.03*	*0.00*	*0.02*	*0.00*	*0.02*	*0.00*	*0.02*
	Shoulder	0.40	*0.00*	0.89	*0.00*	*0.00*	*0.00*	*0.00*	*0.00*	*0.00*	*0.00*	*0.02*	*0.00*	*0.05*	*0.00*	*0.03*	*0.00*
Excitation level	Wrist	0.26	0.60	0.26	0.72	0.27	0.75	0.11	*0.03*	0.97	0.33	0.35	0.89	0.81	0.66	0.49	0.32
	Elbow1	0.11	0.60	*0.02*	0.16	*0.02*	0.34	0.29	0.16	*0.02*	*0.00*	0.56	*0.00*	0.25	*0.00*	*0.02*	0.37
	Elbow2	0.49	0.13	0.43	0.65	*0.01*	0.44	0.53	*0.00*	0.11	0.21	0.97	0.82	0.53	0.11	*0.00*	*0.01*
	Shoulder	0.40	0.08	0.17	0.26	0.79	0.38	0.12	*0.03*	0.40	0.34	0.61	*0.00*	*0.00*	*0.00*	*0.00*	0.73

[a] Bent-arm (P1) posture.
[b] Extended arm (P2) posture.

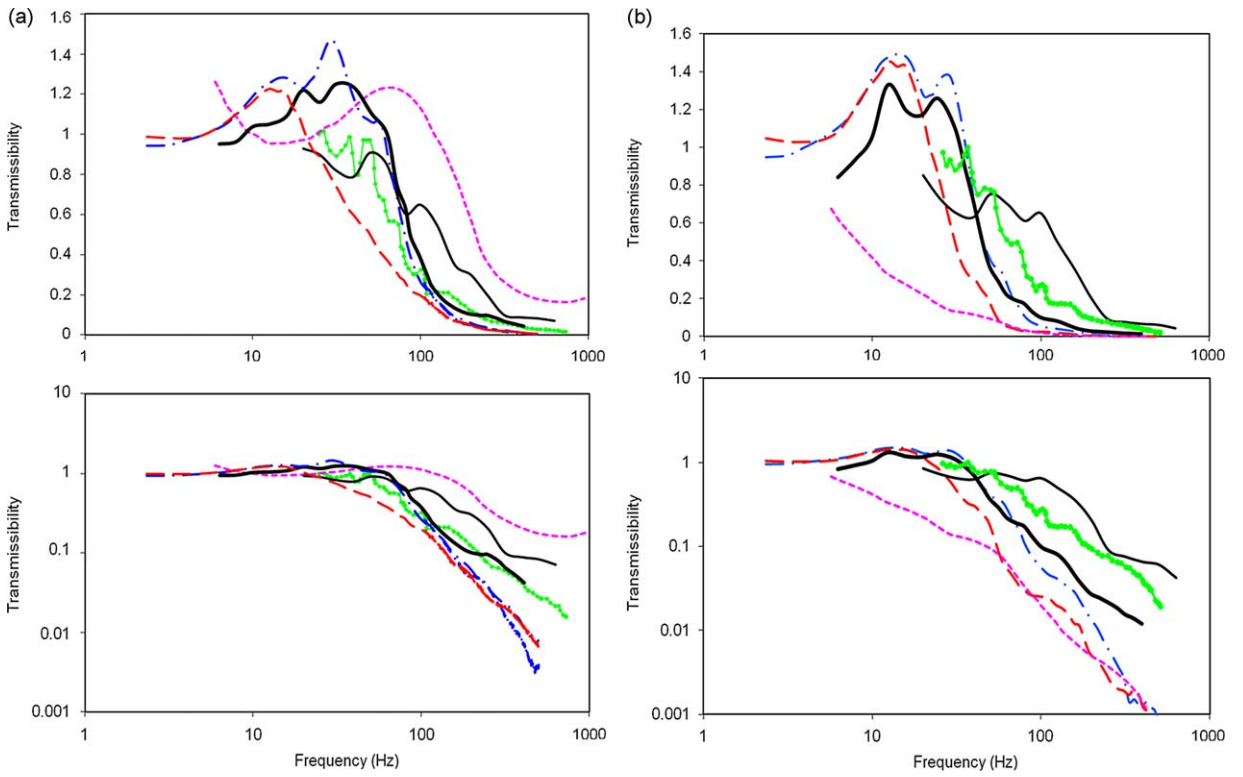

Fig. 7. Comparisons of the measured transmissibility with reported studies: (a) wrist; (b) elbow; Kihlberg [24]; Reynolds and Angevine [26]; Pyykko et al. [27]; Xu et al. [31]; measured-bent-arm; measured-extended arm.

However, there is considerable variability in transmissibility responses compared in Fig. 7, particularly at the elbow. This could be attributed to differences in the accelerometer mounting methods, experimental conditions and subjects' anthropometry. The data reported in [26] show considerable deviation from other data sets. This might be due to the low grip force (18 N) and transmissibility computation relative to the acceleration measured at the base of the handle fixture (close to electrodynamic shaker) rather than hand–handle interface. It has been shown that handle dynamics have significant effect on measurements performed at the base of the handle fixture [38]. Other studies in Fig. 7 computed transmissibility relative to the acceleration measured close to the handle–hand interface with grip force in the 30–50 N range.

3.5. *Effect of grip force*

The magnitudes of transmitted vibration, particularly at frequencies below 200 Hz, are influenced by variations in the grip force, as seen in Tables 3 and 4. Figs. 8 and 9 illustrate the mean transmissibility measured at the wrist, elbow 1 and the shoulder along the z_h- and y_h-axis, respectively, for the three grip forces (10, 30 and 50 N) and two postures (bent-arm (P1) and extended arm (P2)) considered in the study. The results are presented for a constant push force of 50 N. In general, an increase in the grip force increases the magnitude of vibration transmitted to all locations along the z_h-axis for both postures. This trend is also evident in the y_h-axis vibration for the P2 extended arm posture, while an opposite trend can be observed for y_h-axis elbow E1 and shoulder transmissibility under the P1 bent arm posture. The effect of the grip force on the y_h-axis vibration transmitted to the elbow E1 and the shoulder for the P1 posture, however, is relatively small ($p > 0.05$ in most of the frequency range). The characteristic frequencies corresponding to prominent peaks also increase with an increase in the grip force. For the P1 posture, a change in the grip force yields negligible effect on the z_h-axis vibration transmitted along the wrist and the shoulder in the 2.5–15 Hz range ($p > 0.05$ in Table 3) but yields an increase in the vibration magnitudes and characteristic frequencies above 15 Hz ($p < 0.05$). The influence of the grip force on the wrist and elbow E1 transmissibility magnitudes is more evident in the bent-arm (P1) posture than the extended arm (P2) posture above 15 Hz. This may be attributed to the stiffening of the muscles/tissues and joints in the extended arm posture, which tends to increase both the stiffness and the damping of the hand–arm system. The effect of the grip force on the wrist vibration transmissibility in the y_h-axis seems to be concentrated in the 15–80 Hz frequency range for both the postures. The results in Tables 3 and 4 also suggest more important effect of the grip force on the wrist and elbow E1 transmissibility

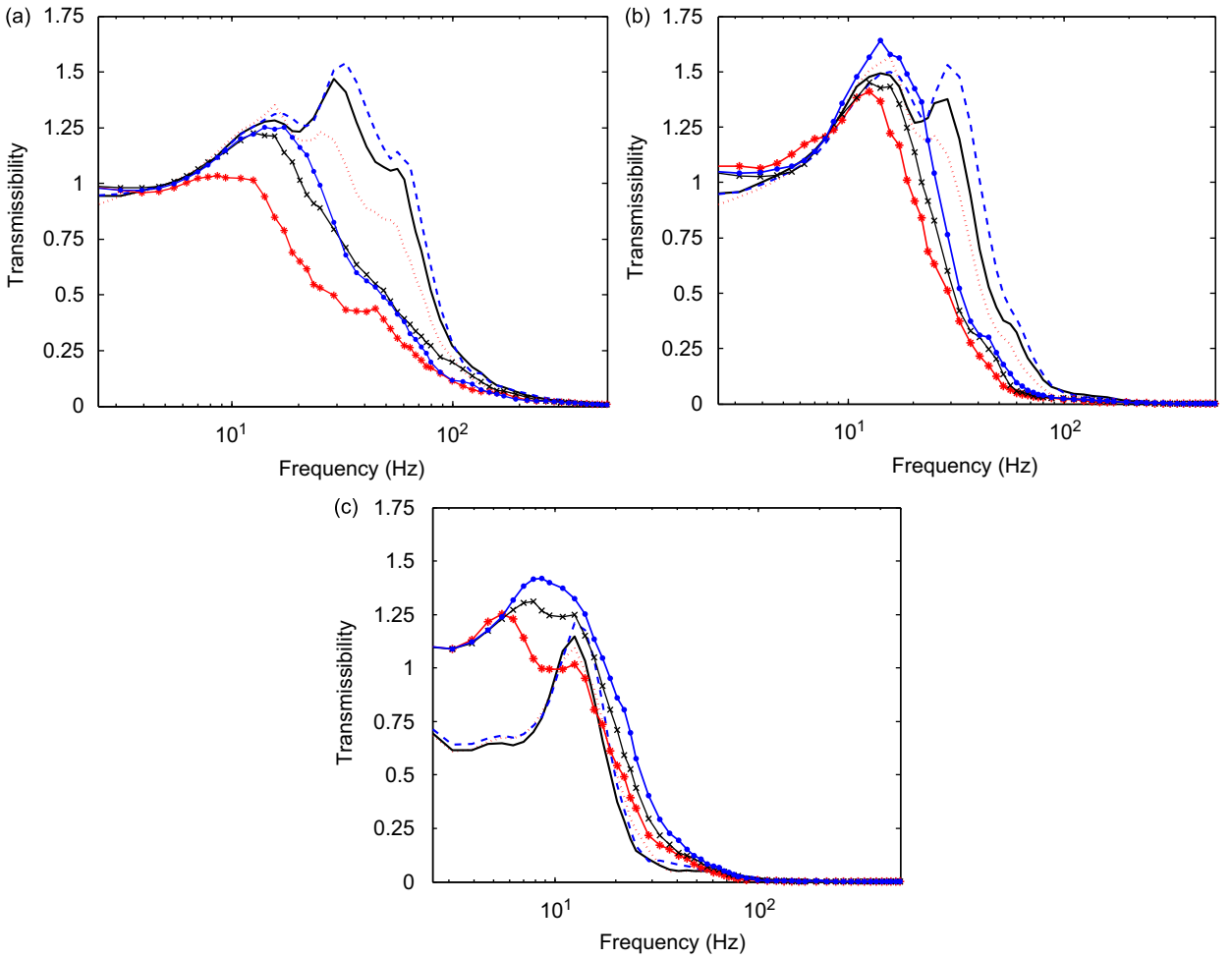

Fig. 8. Effect of grip force on the z_h-axis transmissibility under both postures (different F_g when F_p=50 N, a_{hw}=5.25 ms^{-2}): (a) wrist; (b) elbow 1; (c) shoulder; 10 N-P1; 30 N-P1; 50 N-P1; 10 N-P2; 30 N-P2; 50 N-P2.

(forearm). This tendency was also noted by the subjects who reported higher physical stress and vibration of the forearm under higher grip forces.

The effect of grip force on the most prominent characteristic frequency and z_h-axis transmissibility was further quantified under the bent-arm posture in terms of percentage variations. The results showed that an increase in the grip force from 10 to 50 N (400%) produced a maximum increase of 6.3 Hz (25.0%) in the characteristic frequency of the wrist transmissibility, corresponding to the most prominent peak (around 25 Hz) and a maximum increase of 0.32 (26.4%) in elbow (E2) transmissibility.

3.6. *Effect of push force*

Figs. 10 and 11 illustrate the influence of push force F_p on the transmissibility at the wrist, elbow and the shoulder along the z_h- and y_h-axis, respectively, for both the postures. The influence of F_p on transmitted vibration in the z_h- and y_h-axis at the wrist and elbow is similar to the effect of the grip force above 25 Hz. An increase in the push force, however, tends to decrease wrist and elbow transmissibility in both axes for the bent-arm (P1) posture at frequencies below 25 Hz. This suggests nonlinearity of the human hand–arm system under push force in the low frequency region (below 25 Hz). This kind of behavior, however, cannot be detected from statistical analysis. Figs. 10 and 11 show that the push force considerably affects the shoulder transmissibility for the extended arm (P2) postures in both z_h- and y_h-axis over the majority of the frequency, while Tables 3 and 4 show significant effect of push force ($p < 0.05$) above 15 Hz. The pronounced effect of push force on the shoulder transmissibility under the extended arm posture could be attributed to greater stiffness of both the muscles/tissues and joints with an increase in the push force, and a greater reaction force at the shoulder.

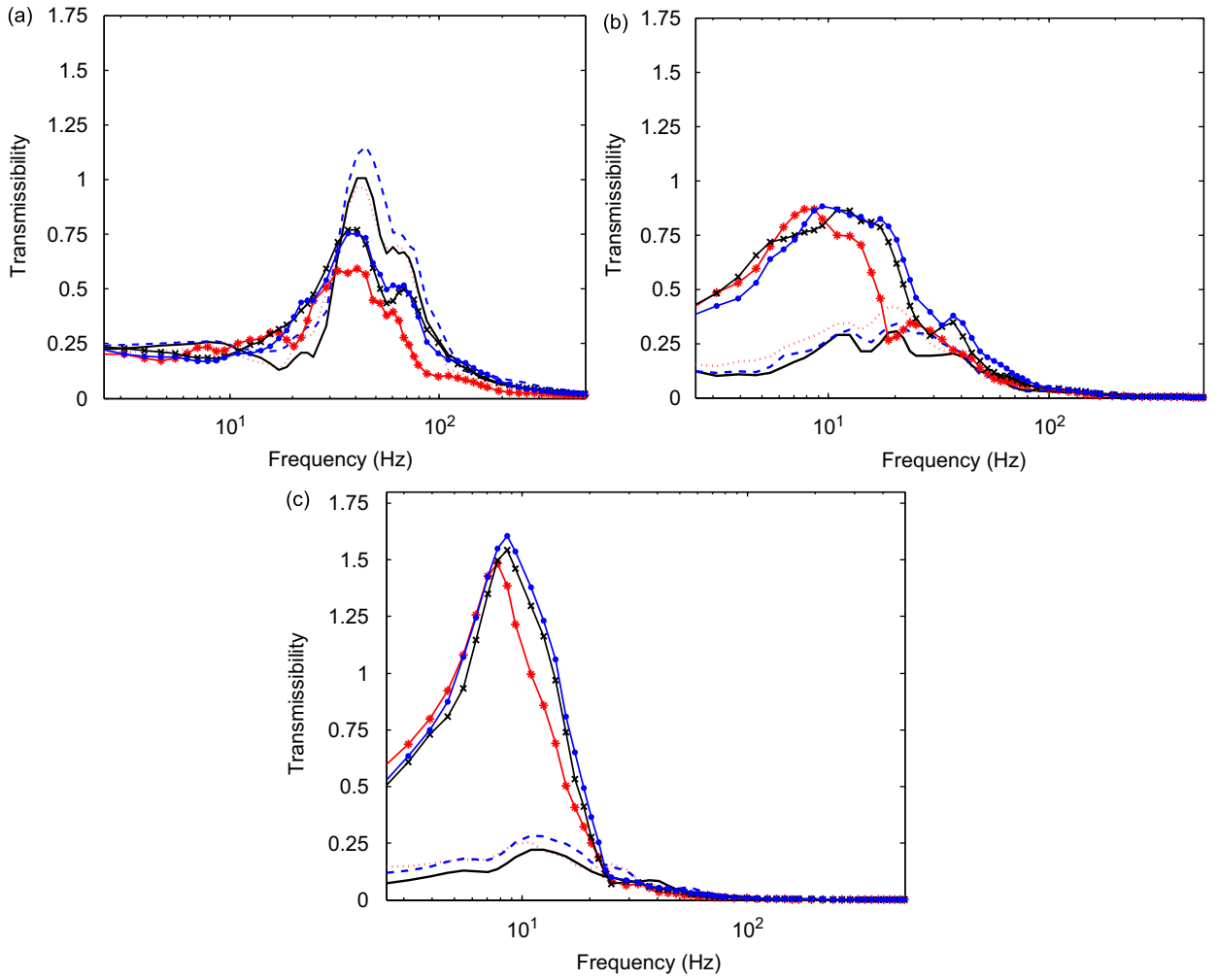

Fig. 9. Effect of grip force on the y_h-axis transmissibility under both postures (different F_g when F_p=50 N, a_{hw}=5.25 ms^{-2}): (a) wrist; (b) elbow 1; (c) shoulder; 10 N-P1; 30 N-P1; 50 N-P1; 10 N-P2; 30 N-P2; 50 N-P2.

The effect of push force on the measured responses was further evaluated in terms of percent change in the most prominent characteristic frequency and the z_h-axis transmissibility for the bent-arm (P1) posture. The results showed that an increase in the push force from 25 to 75 N (200%) yields a maximum increase of 3.9 Hz (33.3%) in the characteristic frequency corresponding to the most prominent peak (around 11.0–15.6 Hz) in elbow 2 transmissibility and a maximum increase of 0.085 (31.86%) in the transmissibility at elbow 1. The results in Figs. 8–11, and Tables 3 and 4 suggest that the grip force mostly affects the dynamic characteristics (transmissibility and resonant frequencies) of the forearm, while the push force affects the dynamic characteristics of the entire hand–arm system. This observation agrees with the deduction on the effects of hand forces on the impedance magnitude reported in [41].

3.7. *Effect of excitation magnitude*

The influence of excitation magnitude on the transmissibility responses measured at the wrist, elbow 1 and the shoulder along the z_h- and y_h-axis are presented in Figs. 12 and 13, respectively. The results are presented for the two postures corresponding to F_g=30 N and F_p=50 N. The excitation with overall frequency-weighted magnitudes of 2.65 and 5.25 ms^{-2} are denoted as "low" and "high", respectively, in the figures. The figures show that excitation magnitude affects transmissibility, particularly around the characteristic frequencies. In the direction of excitation (z_h-axis), an increase in excitation magnitude generally resulted in an increase in the transmissibility in the low frequency region (below 15 Hz), while a decrease in the wrist and elbow E1 transmissibility occurred at frequencies above 70 and 25 Hz, respectively. This observation suggests nonlinear effect of excitation magnitude on the transmissibility. The results of ANOVA presented in Tables 3 and 4 also show the influence of excitation magnitude to be significant ($p < 0.05$) at some frequencies for both the postures. In the z_h-axis (Table 3), the influence of excitation magnitude is significant at all measurement locations only at

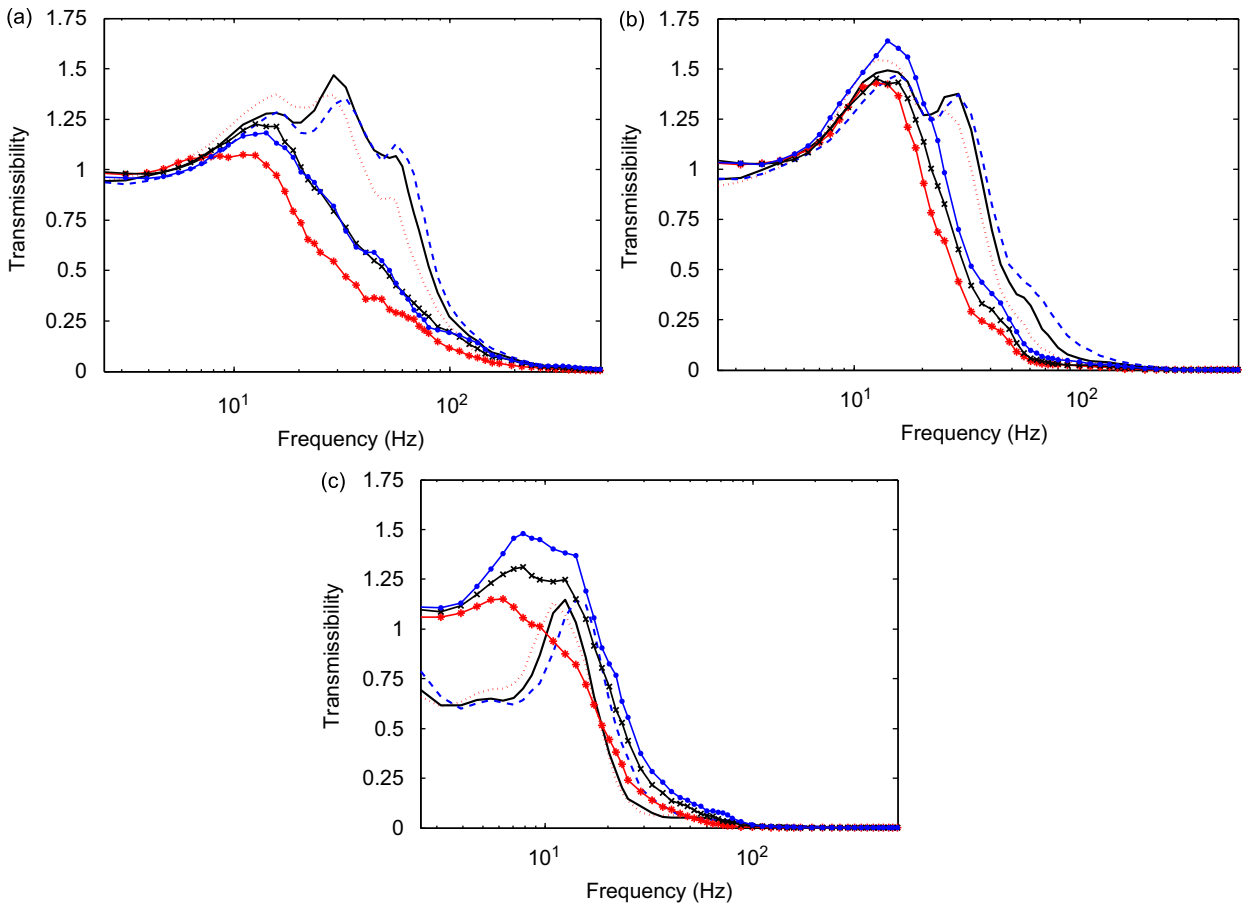

Fig. 10. Effect of push force on z_h-axis transmissibility under both postures (different F_p when F_g=30 N, a_{hw}=5.25 ms^{-2}): (a) wrist; (b) elbow 1; (c) shoulder; 25 N-P1; 50 N-P1; 75 N-P1; 25 N-P2; 50 N-P2; 75 N-P2.

some frequencies. In the y_h-axis, however, the influence on the wrist transmissibility is mostly insignificant ($p > 0.05$) except near 28.9 Hz for the extended arm (P2) posture. The statistical significance of the influence of excitation magnitude is observed to be small compared to the influence of the hand forces.

The peak deviations in the mean transmissibility due to two excitation magnitudes at each measurement location were computed and summarized in Table 5 together with the mean response and the frequency at which the peak deviation occurred. The results are presented for both the postures, and F_g=30 N and F_p=50 N. The results show peak deviation of 0.36 in the y_h-axis transmissibility under the extended arm (P2) posture and 0.18 in the z_h-axis transmissibility under the bent-arm (P1) posture, both occurring at the elbow (E2) location at low frequencies. The observed peak deviations for the P1 posture are lower than the standard deviations of the data acquired during repeatability test (0.23), reproducibility test (0.35), and inter-subject variability (0.38) for comparable hand forces. The peak deviations due to the effect of excitation magnitudes in the data under the P2 posture, however, are considerably larger. These suggest that the effect of excitation level on the z_h-axis transmissibility under the P1 posture is small compare to that under the P2 posture. This could be attributed to the observation made in Figs. 5 and 6, which shows that the human hand–arm system amplifies vibration in the extended arm posture (P2), while it attenuates vibration in the bent-arm posture (P1) below 25 Hz. The effects of excitation magnitude on the y_h-axis transmissibility are also evident under both postures, as seen in Fig. 13.

Somewhat contradictory findings have been reported on the effects of excitation magnitudes on transmissibility [27,29,30]. Two studies have reported that a 10 dB increase in the excitation magnitude increases the transmissibility by 8–10 dB at all frequencies [27,30], while a single study [29] reported negligible influence of excitation magnitude on the wrist transmissibility. A careful examination of the results presented in [29], however, revealed notable effect of excitation magnitude on the imaginary part of the transmissibility response, particularly around the characteristic frequencies. The three studies however considered different hand–arm postures involving elbow angles of 120°, 150° and 180°, which are somewhat close to the extended arm posture used in this study. Unlike the results reported in [27,30], the effect of excitation level on the transmitted vibration was investigated in [29] through analysis of the imaginary part of the transmissibility response obtained for only one subject. The differences in the methodology used in the reported studies may be responsible for the different observations in view of the excitation level effects. The results of the present study

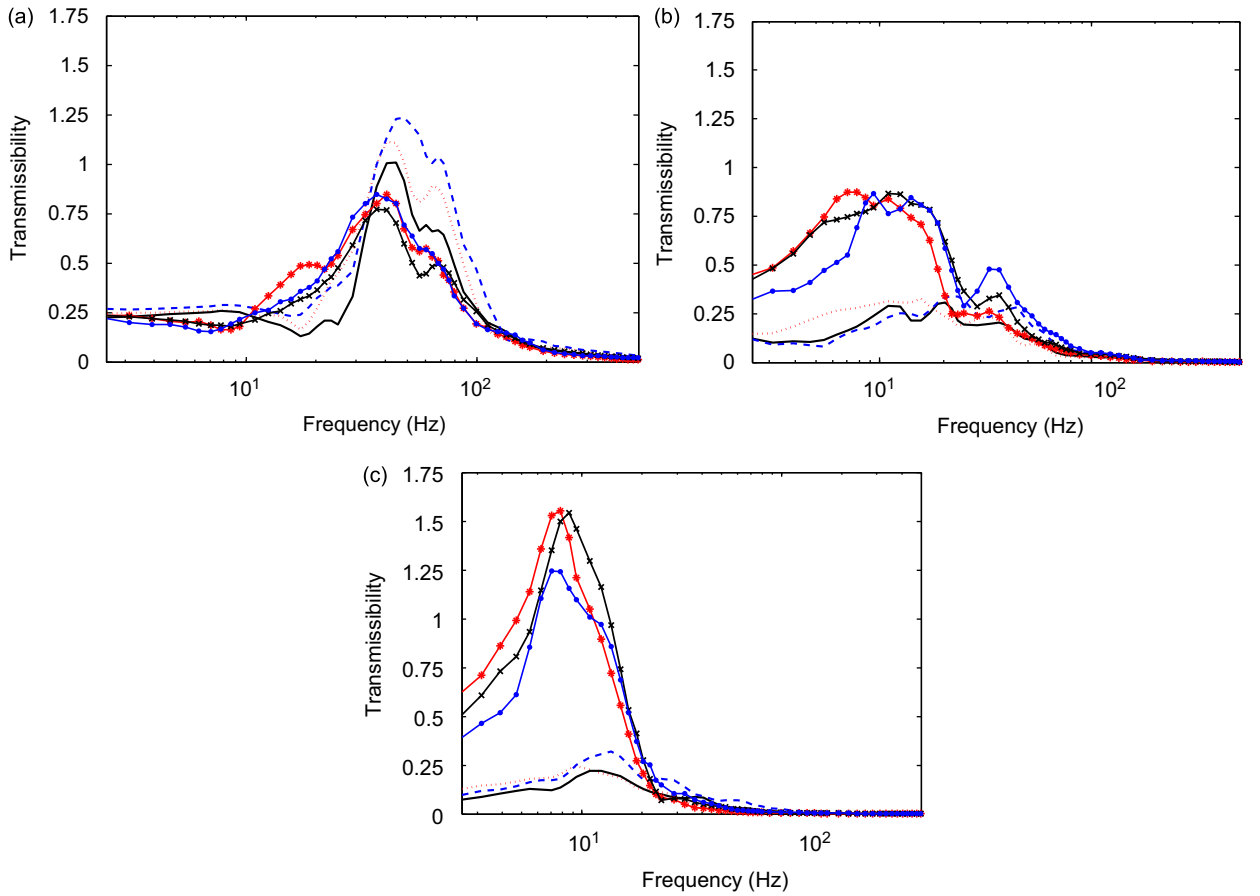

Fig. 11. Effect of push force on y_h-axis transmissibility under both postures (different F_p when F_g=30 N, a_{hw}=5.25 ms^{-2}): (a) wrist; (b) elbow 1; (c) shoulder; 25 N-P1; 50 N-P1; 75 N-P1; 25 N-P2; 50 N-P2; 75 N-P2.

exhibit only partial agreements with the findings reported in [27,30], that the variations in the excitation magnitude affect the transmissibility responses, but disagree that the increase in transmissibility magnitude is the same in the entire frequency range. The results presented in Figs. 12 and 13 and Tables 3 and 4 show pronounced effects of excitation magnitude around the vicinity of the characteristic frequencies, which was also observed from the data reported in [29].

3.8. *Brief discussion on potential model development and injury assessment applications*

The operators of hand-held power tools may assume hand–arm posture that lies in-between the bent and fully extended arm. The results of this study have shown that the nature of vibration transmitted to the forearm, upper-arm and shoulder would strongly depend upon the hand–arm posture. Therefore, the measured transmissibility responses could be used to derive hand–arm mechanical-equivalent models on the basis of posture, and distributed transmissibility responses at the wrist, elbow and shoulder. These models could yield more reliable estimate of vibration power absorbed in different segments of the human hand–arm system than models based upon the localized driving-point mechanical impedance. It has been suggested that there is a relationship between the quantity of vibration energy absorbed in the hand–arm system and the risks of occurrence of vibration injury [43]. The estimated vibration absorbed power of different segments of the hand–arm may yield reliable assessment of musculoskeletal disorders. The following observations raise questions on the validity of the mechanical-equivalent models with fixed shoulder: (i) the observed high low frequency vibration of the shoulder in the extended arm posture observed in this study; and (ii) the reported high vibration of the head in the 12.5–16 Hz under extended arm posture [30]. Furthermore, the transmissibility responses of different segments (wrist, elbow and shoulder) reported in this study could be used, using the methods suggested in [31], to derive appropriate frequency-weightings for assessment of potential injury risk associated with different segments of the human hand–arm system.

The frequency-weighting defined in ISO 5349-1 standard [19] has been widely used in assessing vascular and neurological components of the hand–arm vibration syndrome (vibration-induced white fingers), which are generally high frequency phenomenon. The recommended frequency-weighting, however, yields significant attenuation at frequencies above 12.5 Hz. Although the tool vibration at frequencies above 100 Hz is mostly confined to the hand, greater magnitude

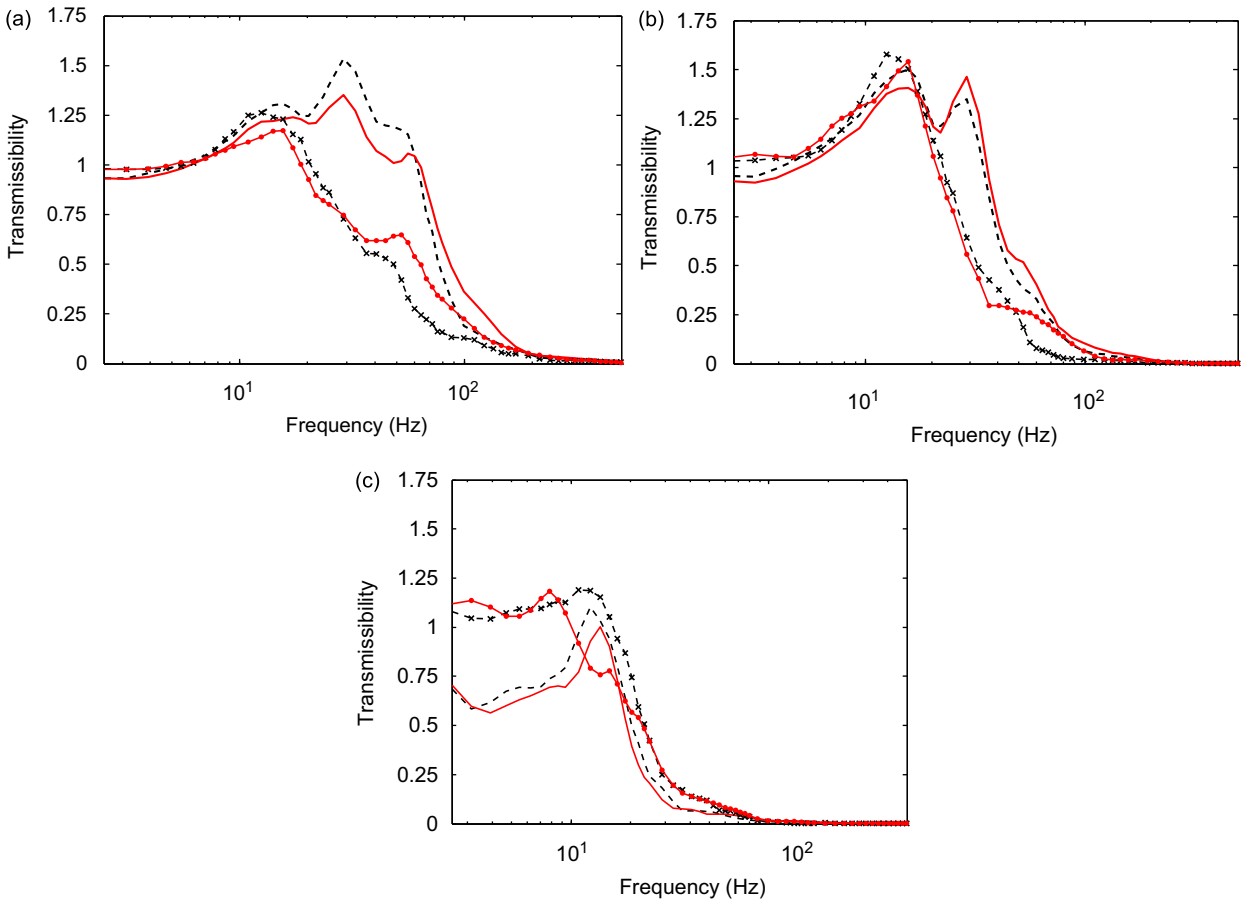

Fig. 12. Effect of excitation level on the z_h-axis transmissibility under both postures (F_g=30 N, F_p=50 N): (a) wrist; (b) elbow 1; (c) shoulder; – – – – high-P1; low-P1; high-P2; low-P2.

of low frequency (below 25 Hz) vibration are transmitted to the forearm and beyond, which may lead to rapid muscles/tissues fatigue and musculoskeletal disorders. Therefore, hand–arm vibration syndrome (HAVS) predicted based on the standard could be largely different from what was observed from epidemiological studies [44,45]. The current ISO standard [19] relates potential injury risks due to hand-transmitted vibration to vibration magnitude, usually measured on the tool's handle, frequency-weighting and exposure duration. Some studies have suggested that the current ISO frequency-weighting is acceptable for approximately assessing the overall discomfort and some disorders in the wrist and arms, while the weighting is unlikely to be suitable for assessing hand disorders [36,46]. Alternative weightings are therefore required for the assessment of different components of HAVS.

Considering the important effects of hand–arm posture and transmission of low frequency vibration to the forearm and beyond revealed by the results of this study, it may be more appropriate to define two different frequency-weightings for assessment of hand–arm potential injury risks. The first weighing could be associated with the vascular and neurological components (vibration-induced white fingers)—a high frequency vibration phenomenon, while the second could be for musculoskeletal disorder—a low frequency vibration phenomenon.

4. Conclusions

In this study, the z_h-axis handle vibration transmitted to the wrist, elbow (on both forearm and upper-arm sides) and the shoulder of the hand–arm system was measured under two different postures and excitation magnitudes, and different combinations of grip and push forces. The vibration transmissibility, reported in both linear and logarithmic scales, tend to decrease with increasing distance between the measurement location and the source. The linear scale emphasizes low frequency transmissibility, while the logarithmic scale emphasizes high frequency transmissibility; this facilitated identification of characteristic frequencies. The results show that the human hand–arm system in an extended arm posture amplifies the z_h-axis vibration transmitted to the upper-arm and the trunk at frequencies below 25 Hz. Furthermore, this posture attenuates the transmitted vibration more effectively than the bent-arm posture above 25 Hz, except at the shoulder. The results also showed greater y_h-axis transmitted vibration for the extended arm posture than the bent-arm

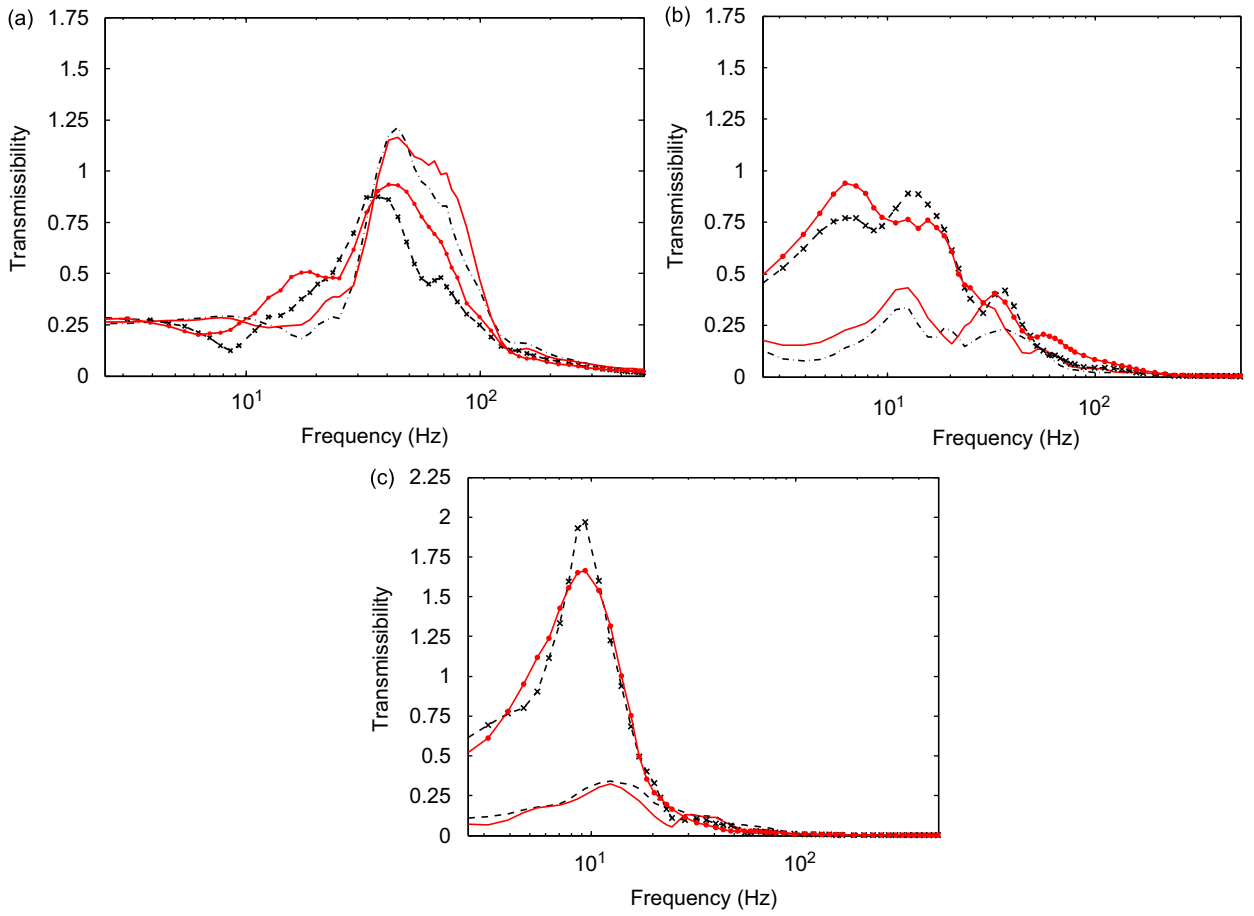

Fig. 13. Effect of excitation level on the y_h-axis transmissibility under both postures (F_g=30 N, F_p=50 N): (a) wrist; (b) elbow 1; (c) shoulder; – – – – high-P1; ——— low-P1; ——×——— high-P2; ——●——— low-P2.

Table 5
Peak standard deviation in transmissibility due to different excitation magnitudes (F_g=30 N, F_p=50 N).

Measurement location	Bent-arm (P1) posture			Extended arm (P2) posture		
	Peak deviation	Mean value	Frequency (Hz)	Peak deviation	Mean value	Frequency (Hz)
Wrist_y_h	0.16	0.94	79.69	0.21	0.49	56.25
Wrist_z_h	0.14	1.12	32.81	0.20	0.42	56.25
Elbow1_y_h	0.11	0.28	28.91	0.12	0.85	6.25
Elbow1_z_h	0.11	0.46	32.81	0.12	1.37	12.50
Elbow2_y_h	0.11	0.33	36.72	*0.36*	0.49	*12.50*
Elbow2_z_h	*0.18*	0.67	*15.63*	0.18	1.21	12.50
Shoulder_y_h	0.09	0.18	25.00	0.21	1.30	9.38
Shoulder_z_h	0.14	0.54	10.94	0.28	0.97	12.50

posture below 25 Hz. This suggests that operators of power tools with frequencies below 25 Hz may experience greater muscles/tissues fatigue and symptoms of musculoskeletal disorder when working with extended arm posture.

The results further showed that variations in the grip force mostly affect the responses of the forearm, while changes in the push force affect the dynamic responses of the entire hand–arm system. The effect of the excitation magnitudes was observed to be significant around the prominent peaks in the transmissibility for both the bent-arm and extended arm postures. The results further showed considerable vibration of the shoulder, this raises concern about the validity of mechanical-equivalent models of the human hand–arm with fixed shoulder. The mean measured transmissibility corresponding to specific grip and push forces and posture may serve as target responses for developing mechanical-equivalent model of the hand–arm system, which may yield reliable estimate of vibration power absorption of different segments of the hand–arm system for injury assessment.

References

[1] J. Friden, Vibration damage to the hand: clinical presentation, prognosis and length and severity of vibration required, *Journal of Hand Surgery* 26B (2001) 471–474.

[2] M. Bovenzi, L. Petronio, F. DiMarino, Epidemiological survey of shipyard workers exposed to hand–arm vibration, *International Archives of Occupational and Environmental Health* 46 (1980) 251–266.

[3] J. Malchaire, B. Maldague, J.M. Huberlant, F. Crouqet, Bone and joint changes in the wrists and elbows and their association with hand and arm vibration exposure, *Annals of Occupational Hygiene* 30 (1986) 461–468.

[4] I. Pyykko, O. Korhonen, M. Farkkila, J. Starck, S. Aatola, V. Jantti, Vibration syndrome among Finnish forest workers, a follow-up from 1972 to 1983, *Scandinavian Journal of Work, Environment & Health* 12 (1986) 307–312.

[5] W. Taylor, Biological effects of the hand–arm vibration syndrome: historical perspectives and current research, *Journal of Acoustics Society of America* 83 (1988) 415–422.

[6] T.J. Partanen, T. Kumlin, M.J. Karvonen, Subjective symptoms connected with exposure of the upper limbs to vibration, *Work Environment & Health* 7 (1970) 80–81.

[7] A.J. Brammer, Dose-response relationships for hand-transmitted vibration, *Scandinavian Journal of Work, Environment & Health* 12 (1986) 284–288.

[8] T. Nilsson, L. Burstrom, M. Hagberg, Risk assessment of vibration exposure and white finger among platters, *International Archives of Occupational and Environmental Health* 61 (1989) 473–481.

[9] M. Bovenzi, Exposure-response relationship in the hand–arm vibration syndrome: an overview of current epidemiology research, *International Archives of Occupational and Environmental Health* 71 (1998) 509–519.

[10] S. Rakheja, C. Rajalingham, P.-É. Boileau, Analysis of hand-transmitted vibration of a hand-held percussive tool, *European Journal of Mechanical and Environmental Engineering* 47 (2002) 141–156.

[11] R. Jahn, M. Hesse, Applications of hand–arm models in the investigation of the interaction between man and machine, *Scandinavian Journal of Work, Environment & Health* 12 (1986) 343–346.

[12] E.V. Golycheva, V.I. Batbitsky, A.M. Veprik, Vibration protection for an operator of a hand-held percussion machine, *Journal of Sound and Vibration* 274 (2004) 351–367.

[13] H. Hiratsukaa, Reducing the physical strain of pneumatic tools, in: S. Kumar (Ed.), *Advances in Occupational Ergonomics and Safety*, IOS Press, 1998, pp. 428–431.

[14] E. Greenslade, T.J. Larsson, Reducing vibration exposure from hand-held grinding, sanding and polishing power tools by improvement in equipment and industrial processes, *Safety Science* 25 (1997) 143–152.

[15] M.J. Griffin, Evaluating the effectiveness of gloves in reducing hazards of hand-transmitted vibration, *Occupational and Environment Medicine* 55 (1998) 340–348.

[16] Y. Aldien, P. Marcotte, S. Rakheja, P.-É. Boileau, Influence of hand–arm posture on biodynamic response of the hand–arm exposed to z_h-axis vibration, *International Journal of Industrial Ergonomics* 36 (2006) 45–59.

[17] R. Gurram, S. Rakheja, G.J. Gouw, Mechanical impedance of the human hand–arm system subject to sinusoidal and stochastic excitations, *International Journal of Industrial Ergonomics* 16 (1995) 135–145.

[18] J.W. Mishoe, C.W. Suggs, Hand–arm vibration part II: vibrational responses of the human hand, *Journal of Sound and Vibration* 53 (1977) 545–558.

[19] ISO-5349-1, Mechanical vibration and shock-measurement and evaluation of human exposure to hand-transmitted vibration-part 1—general requirements, 2001.

[20] M.J. Griffin, Foundations of hand-transmitted vibration standards, *Nagoya Journal of Medical Science* 57 (1994) 147–164.

[21] S. Rakheja, J.Z. Wu, R.G. Dong, A.W. Schopper, A comparison of biodynamic models of the human hand–arm for applications to hand-held power tools, *Journal of Sound and Vibration* 249 (2002) 55–82.

[22] F. Scarpa, J. Giacomin, Y. Zhang, P. Pastorino, Mechanical performance of auxetic polyureathane for antivibration gloves applications, *Cellular Polymers* 24 (2005) 253–268.

[23] P. Marcotte, Y. Aldien, P.-É. Boileau, S. Rakheja, J. Boutin, Effect of handle size and hand–handle contact force on the biodynamic response of the hand–arm system under z_h-axis vibration, *Journal of Sound and Vibration* 283 (2005) 1071–1091.

[24] S. Kihlberg, Biodynamic response of the hand–arm system to vibration from an impact hammer and a grinder, *International Journal of Industrial Ergonomics* 16 (1995) 1–8.

[25] B.P. Kattel, J.E. Fernandez, The effect of rivet gun on hand–arm vibration, *International Journal of Industrial Ergonomics* 23 (1999) 595–608.

[26] D.D. Reynolds, E.N. Angevine, Hand–arm vibration. Part II: vibration transmission characteristics of the hand and arm, *Journal of Sound and Vibration* 51 (1977) 255–265.

[27] I. Pyykko, M. Farkkila, J. Toivanen, O. Korhonen, J. Hyvarinen, Transmission of vibration in the hand–arm system with special reference to changes in compression and acceleration, *Scandinavian Journal of Work, Environment & Health* 2 (1976) 87–95.

[28] T. Cherian, S. Rakheja, R.B. Bhat, An analytical investigation of an energy flow divider to attenuate hand-transmitted vibration, *International Journal of Industrial Ergonomics* 17 (1996) 455–467.

[29] S. Aatola, Transmission of vibration to the wrist and comparison of frequency response function estimators, *Journal of Sound and Vibration* 131 (1989) 497–507.

[30] H. Sakakibara, T. Kondo, M. Miyao, S. Yamada, T. Nakagawa, F. Kobayashi, Y. Ono, Transmission of hand–arm vibration to the head, *Scandinavian Journal of Work Environment & Health* 12 (1986) 359–361.

[31] X.S. Xu, D.E. Welcome, T.W. Mcdowell, C. Warren, R.G. Dong, An investigation on characteristics of the vibration transmitted to the wrist and elbow in the operation of impact wrenches, *International Journal of Industrial Ergonomics* 39 (2008) 174–184.

[32] D.D. Reynolds, R.J. Falkenberg, A study of hand vibration on chipping and grinding operators, part I: four-degree-of-freedom lumped parameter model of the vibration response of the human hand, *Journal of Sound and Vibration* 95 (1984) 499–514.

[33] International Standards Organization ISO-10068, Mechanical vibration and shock-free mechanical impedance of the human hand–arm system at the driving point, 1998.

[34] R. Gurram, S. Rakheja, A.J. Brammer, Driving-point mechanical impedance of the human hand–arm system: synthesis and model development, *Journal of Sound and Vibration* 180 (1995) 439–458.

[35] R.G. Dong, D.E. Welcome, T.W. McDowell, J.Z. Wu, A.W. Schopper, Frequency weighting derived from power absorption of fingers–hand–arm system under z_h-axis vibration, *Journal of Biomechanics* 39 (2006) 2311–2324.

[36] J.H. Dong, R.G. Dong, S. Rakheja, D.E. Welcome, T.W. McDowell, J.Z. Wu, A method for analyzing absorbed power distribution in the hand and arm substructures when operating vibration tools, *Journal of Sound and Vibration* 311 (2008) 1286–1304.

[37] R.G. Dong, J.Z. Wu, T.W. McDowell, D.E. Welcome, A.W. Schopper, Distribution of mechanical impedance at the fingers and the palm of the human hand, *Journal of Biomechanics* 38 (2005) 1165–1175.

[38] S.A. Adewusi, S. Rakheja, P. Marcotte, P.-E. Boileau, On the discrepancies in the reported human hand–arm impedance at higher frequencies, *International Journal of Industrial Ergonomics* 38 (2008) 703–714.

[39] C. Devriendt, P. Guillaume, Identification of modal parameters from measurements, *Journal of Sound and Vibration* 314 (2008) 343–356.

[40] C. Devriendt, P. Guillaume, The use of transmissibility measurements in output-only modal analysis, *Mechanical Systems and Signal Processing* 21 (2007) 2689–2696.

[41] S. Adewusi, S. Rakheja, P. Marcotte, P.-E. Boileau, J. Boutin, On the human hand–arm resonant frequencies, *Proceedings 11th International Conference on Hand–Arm Vibration*, Bologna, Italy, 3–7 June, 2007, pp. 341–348.
[42] INTERNATIONAL STANDARD ORGANIZATION, ISO-10819, Mechanical vibration and shock—hand–arm vibration—method for the measurement and evaluation of the vibration transmissibility of gloves at the palm of the hand, 1996.
[43] I.M. Lindstrom, Vibration injury in rock drillers chiselers, and grinders, some views on the relationship between the quantity of energy and the risk of occurrence of vibration injury, *Proceedings of International Conference on Hand–arm Vibration*, Cincinnati, USA, 1977, pp. 77–83.
[44] T. Nilsson, L. Burström, M. Hagberg, Risk assessment of vibration exposure and white fingers among platers, *International Archives of Occupational and Environmental Health* 61 (1989) 473–481.
[45] P.L. Pelmear, D. Leong, W. Taylor, M. Nagalingam, D. Fung, Measurement of vibration of hand-held tools: weighted or unweighted?, *Journal of Occupational Medicine* 31 (1989) 902–908
[46] M. Griffin, M. Bovenzi, C.M. Nelson, Dose-response patterns for vibration-induced white finger, *Occupational and Environmental Medicine* 60 (2003) 16–26.
[47] R. Ho, *Handbook of Univariate and Multivariate Data Analysis and Interpretation Using SPSS*, Chapman and Hall/CRC, Florida, 2006.
[48] M. Kutner, C.J. Nachtsheim, J. Neter, W. Li, *Applied Linear Statistical Models*, McGraw Hill, Irwan, New York, 2005.